Electronic Supplementary Material (ESI) for Physical Chemistry Chemical Physics.

Supplementary Information

Improved ion adsorption capacities and diffusion dynamics in surface anchored $MoS_2 \perp Mo_{4/3}B_2$ and $MoS_2 \perp Mo_{4/3}B_2O_2$ heterostructures as the anodes for alkaline metal ion batteries

Zifeng Song[1], Haoliang Liu[1], Baiyi Chen[2], Qin Jiang[1], Fengxiang Sui[1], Kai Wu[1], Yonghong Cheng[1], Bing Xiao[1]*

1.State Key Laboratory of Electrical Insulation and Power Equipment, School of Electrical Engineering, Xi'an Jiaotong University, Xi'an 710049, China

2.State Grid Hebei Economic Research Institute, Shijiazhuang 050021, Hebei Province, China

*Corresponding Author: bingxiao84@xjtu.edu.cn

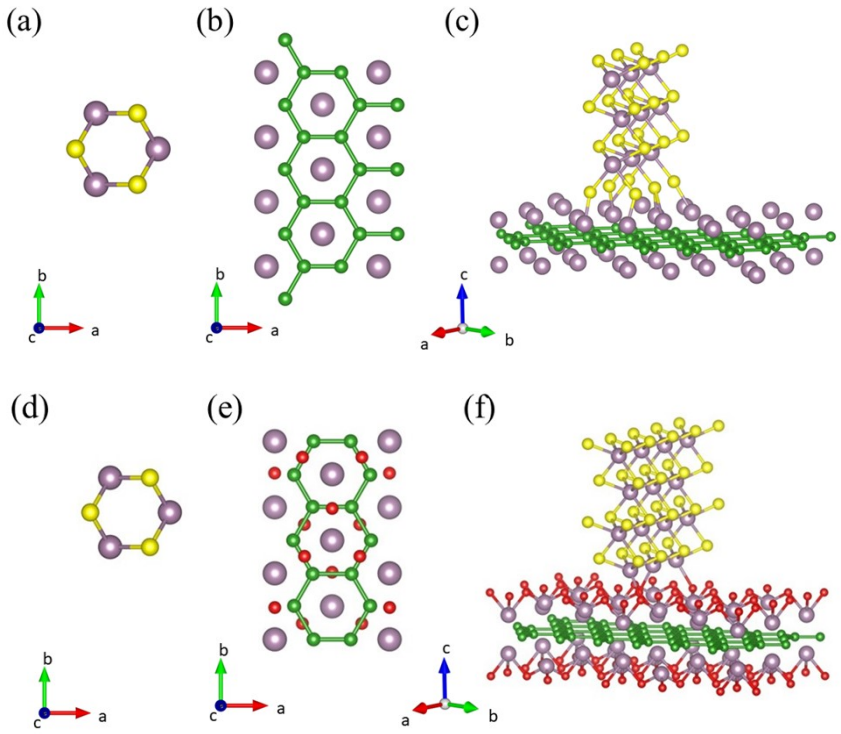

Fig S1 Atomic structures of heterostructures and their constituting components: (a) and (d) The hexagonal structural unit of MoS_2 in the orthogonal unit cell; (b) Atomic structures of $Mo_{4/3}B_2$ in the orthogonal cell; (c) Initial atomic model of $MoS_2 \perp Mo_{4/3}B_2$ heterostructure; (e) Atomic structure of $Mo_{4/3}B_2O_2$ in an orthogonal cell; (f) Initial atomic structure of $MoS_2 \perp Mo_{4/3}B_2O_2$ heterostructure.

(a)

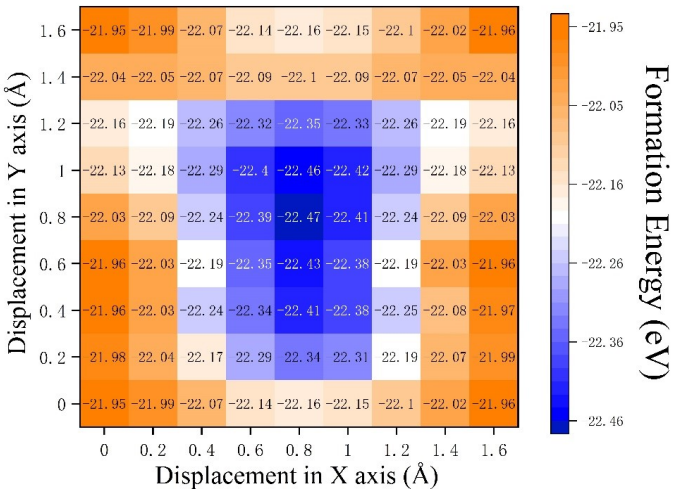

(b)

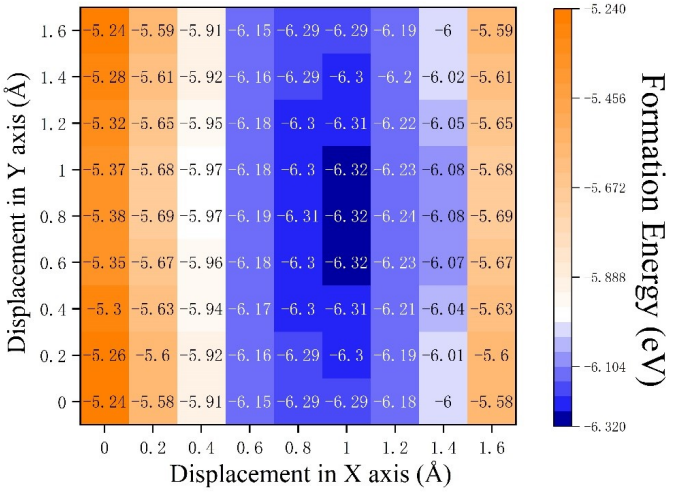

Fig S2 2-D heatmaps of the binding energies for anchoring the MoS_2 nanoflake on the Boridene substrate at various locations. (a) $MoS_2 \perp Mo_{4/3}B_2$; (b) $MoS_2 \perp Mo_{4/3}B_2O_2$.

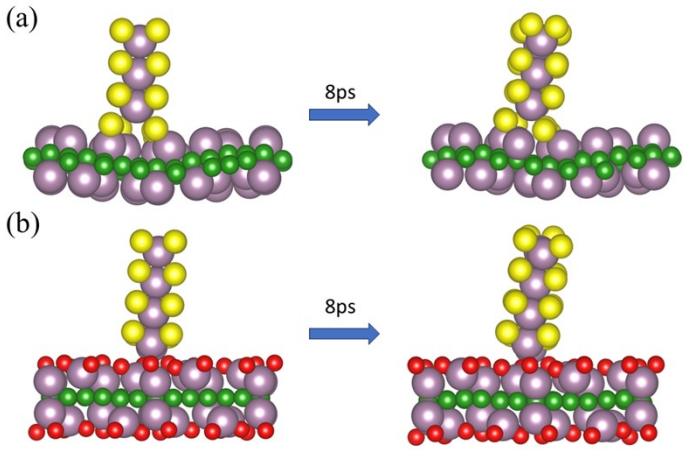

Fig S3 The atomic structures of heterostructures simulated by FPMD at 300K within the NVT ensemble: (a) $MoS_2 \perp Mo_{4/3}B_2$; (b) $MoS_2 \perp Mo_{4/3}B_2O_2$.

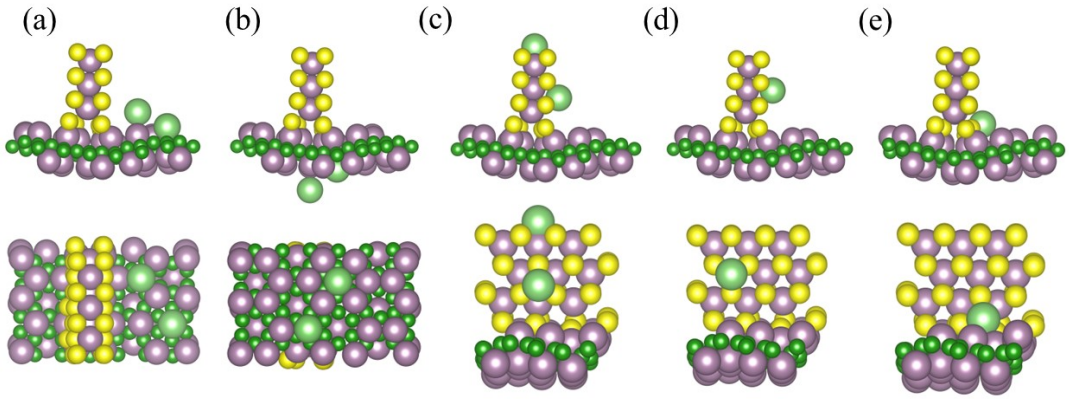

Fig S4 Relaxed atomic structures for the adsorption of Li^+ at various adsorption sites on $MoS_2 \perp Mo_{4/3}B_2$:(a) Hb1 and Tb1 sites; (b) Hb2 and Tb2 sites; (c) Hm and Top sites; (c) Tm site; (d) In site.

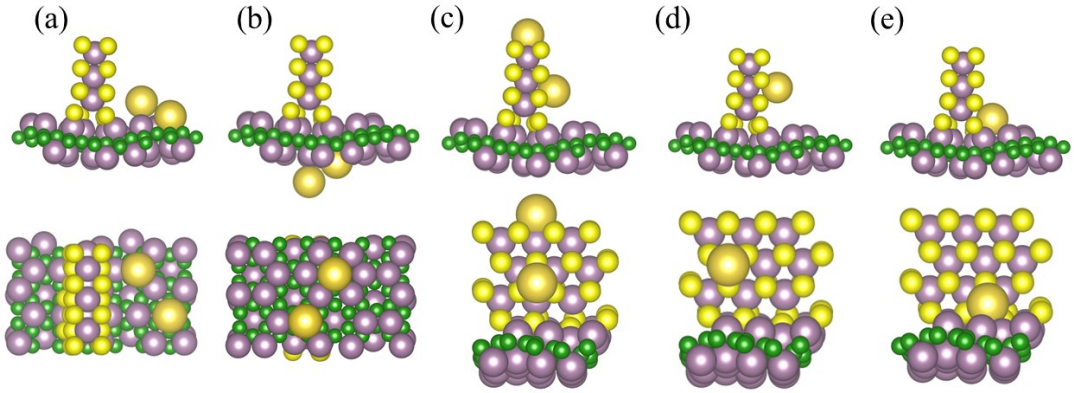

Fig S5 Relaxed atomic structures of the adsorption of Na^+ at different adsorption sites on $MoS_2 \perp Mo_{4/3}B_2$:(a) Hb1 and Tb1 sites; (b) Hb2 and Tb2 sites; (c) Hm and Top sites; (c) Tm site; (d) In site.

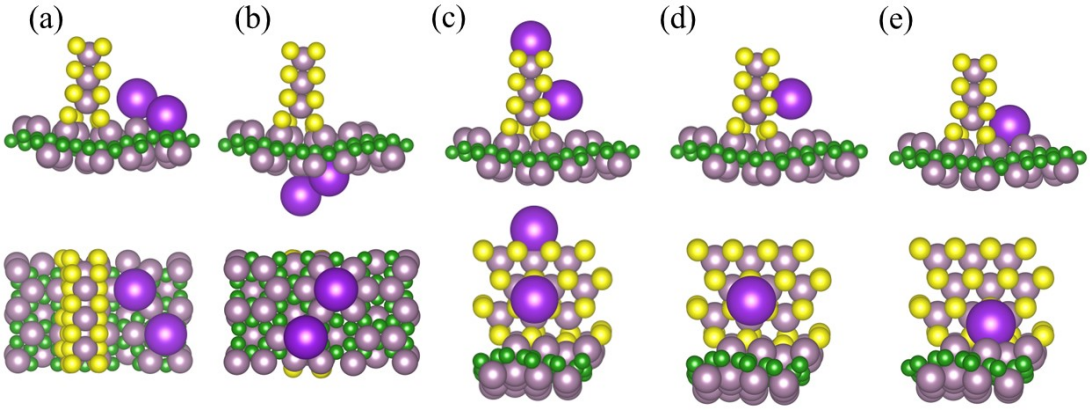

Fig S6 Relaxed atomic structures of the adsorption of K+ ion at various adsorption sites on $MoS_2 \perp Mo_{4/3}B_2$:(a) Hb1 and Tb1 sites; (b) Hb2 and Tb2 sites; (c) Hm and Top sites; (c) Tm site; (d) In site.

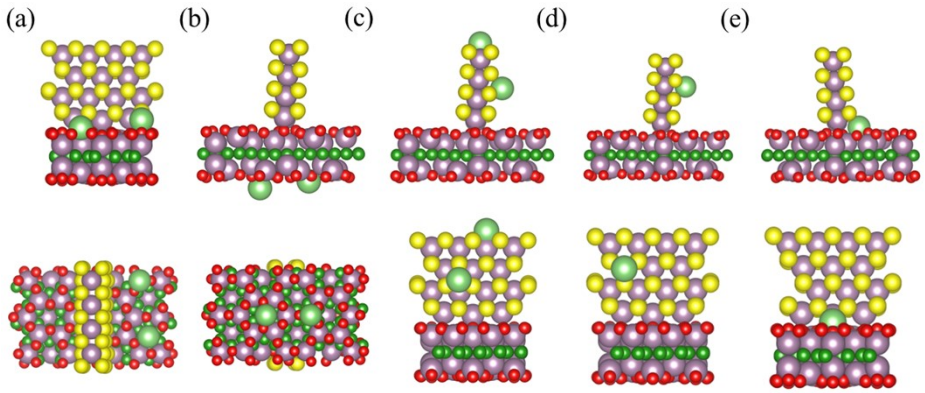

Fig S7 Relaxed atomic structures of the adsorption of Li^+ at various adsorption sites on $MoS_2 \perp Mo_{4/3}B_2O_2$:(a) Hb1 and Tb1 sites; (b) Hb2 and Tb2 sites; (c) Hm and Top sites; (c) Tm site; (d) In site.

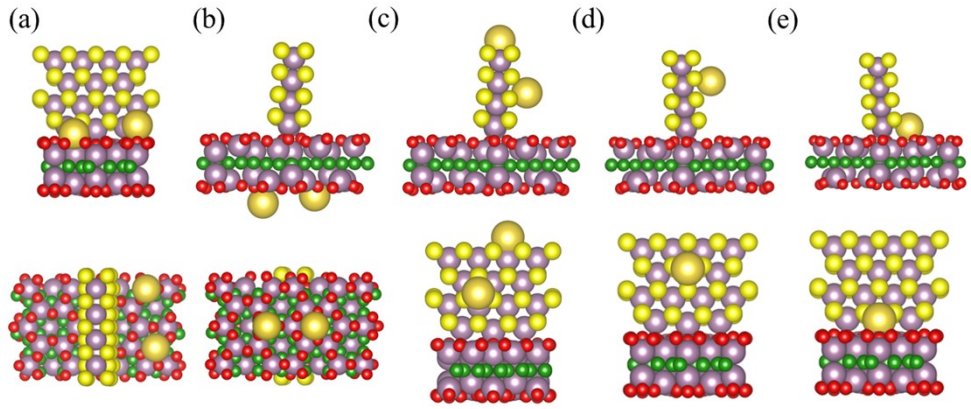

Fig S8 The Optimized atomic structures for adsorbing the Na^+ at different adsorption sites on $MoS_2 \perp Mo_{4/3}B_2O_2$:(a) Hb1 and Tb1 sites; (b) Hb2 and Tb2 sites; (c) Hm and Top sites; (c) Tm site; (d) In site.

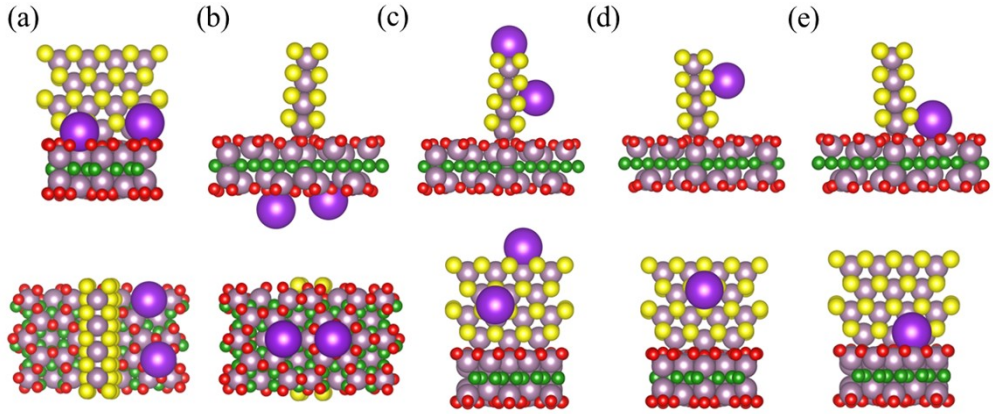

Fig S9 The optimized atomic structures of the adsorption of K^+ at various adsorption sites on $MoS_2 \perp Mo_{4/3}B_2O_2$: :(a) Hb1 and Tb1 sites; (b) Hb2 and Tb2 sites; (c) Hm and Top sites; (c) Tm site; (d) In site.

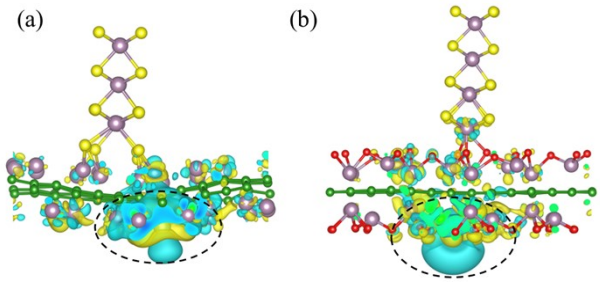

Fig S10 The 3-D contour plots of charge density difference distributions for the adsorption of a single Li^+ ion at Hb2 site on MoS_2 ⊥ $Mo_{4/3}B_2$ and MoS_2 ⊥ $Mo_{4/3}B_2O_2$ heterostructures.

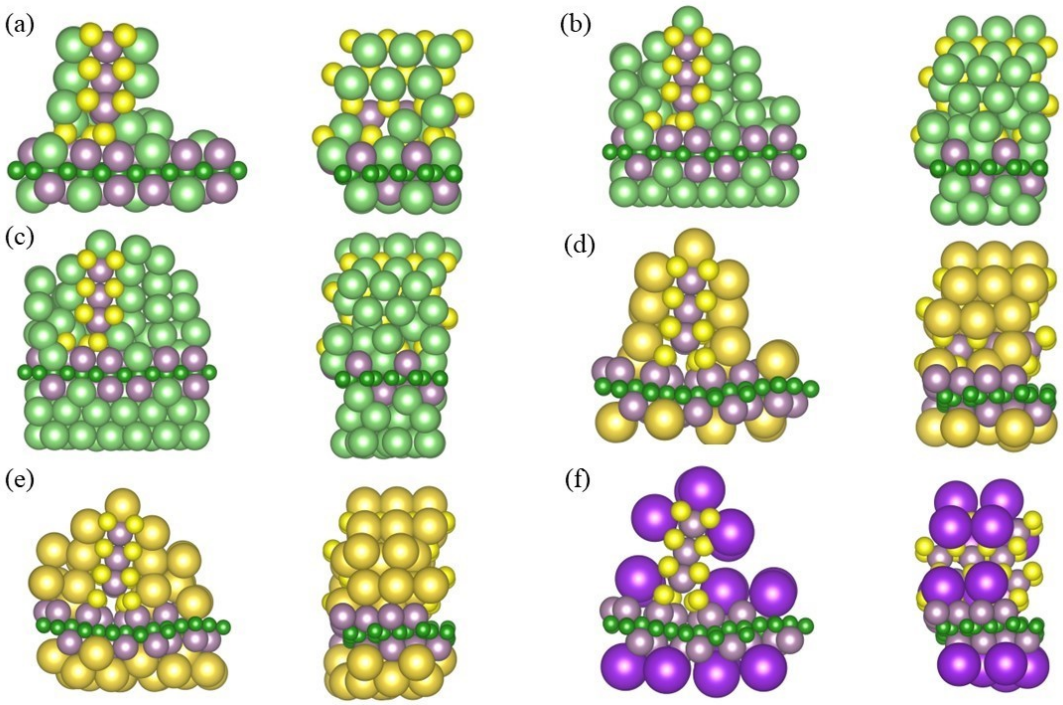

Fig S11 Fully relaxed atomic structures for the formation of full stable absorbate layers on MoS_2 ⊥ $Mo_{4/3}B_2$ hybrid: (a) the first full stable layer of Li^+; (b) the second full stable layer of Li^+; (c) saturation with Li^+; (d) the first full stable layer of Na^+; (e) the second full stable layer of Na^+; (f) the first full stable layer of K^+.

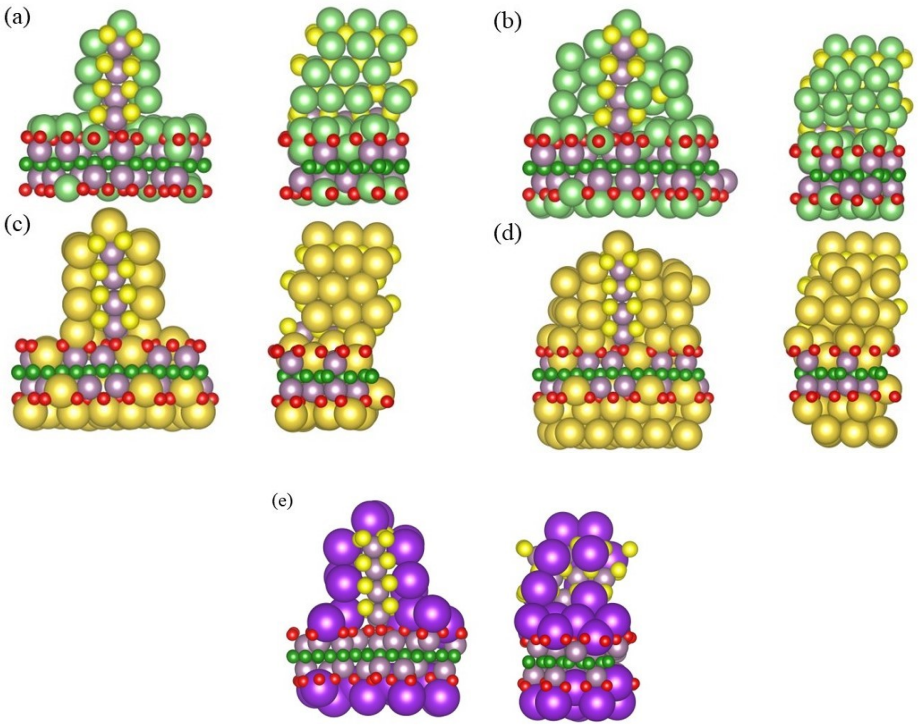

Fig S12 The optimized atomic structures for the formation of full stable adsorption layers on MoS_2 ⊥ $Mo_{4/3}B_2O_2$ hybrid: (a) the first full stable layer of Li^+; (b) fully saturated with Li^+; (c) the first full stable layer of Na^+; (d) the second full stable layer of Na^+; (e) the full stable layer of K^+.

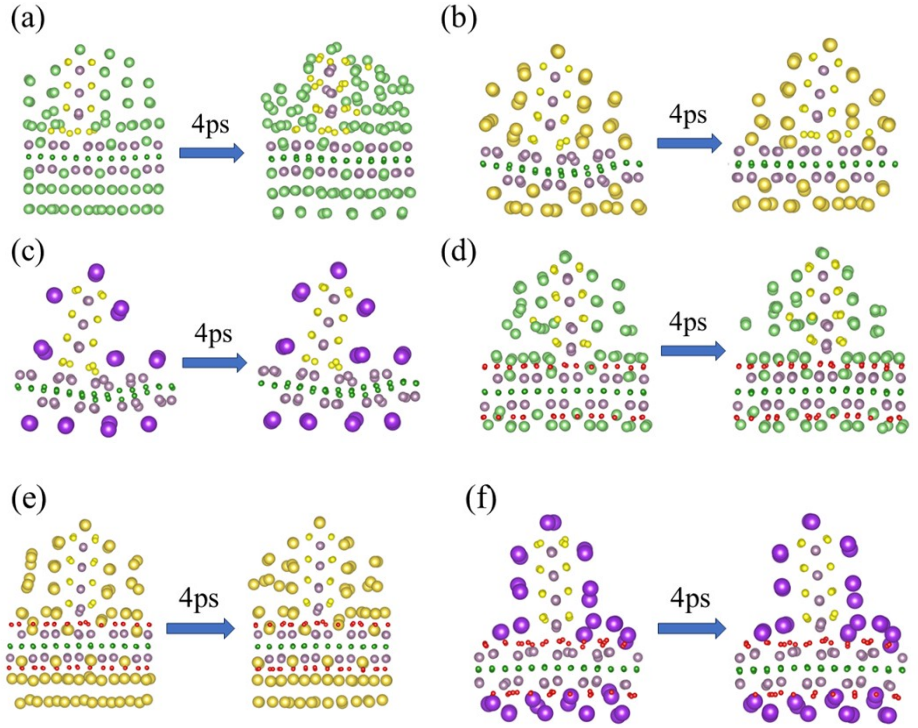

Fig S13 Structural evolutions of alkaline metal ion fully saturated heterostructures simulated by FPMD at 300 K within the NVT ensemble: (a) Li-MoS_2 ⊥ $Mo_{4/3}B_2$; (b) Na-MoS_2 ⊥ $Mo_{4/3}B_2$; (c) K-MoS_2 ⊥ $Mo_{4/3}B_2$; (d) Li-MoS_2 ⊥ $Mo_{4/3}B_2O_2$; (e) Na-MoS_2 ⊥ $Mo_{4/3}B_2O_2$; (f) K-MoS_2 ⊥ $Mo_{4/3}B_2O_2$.

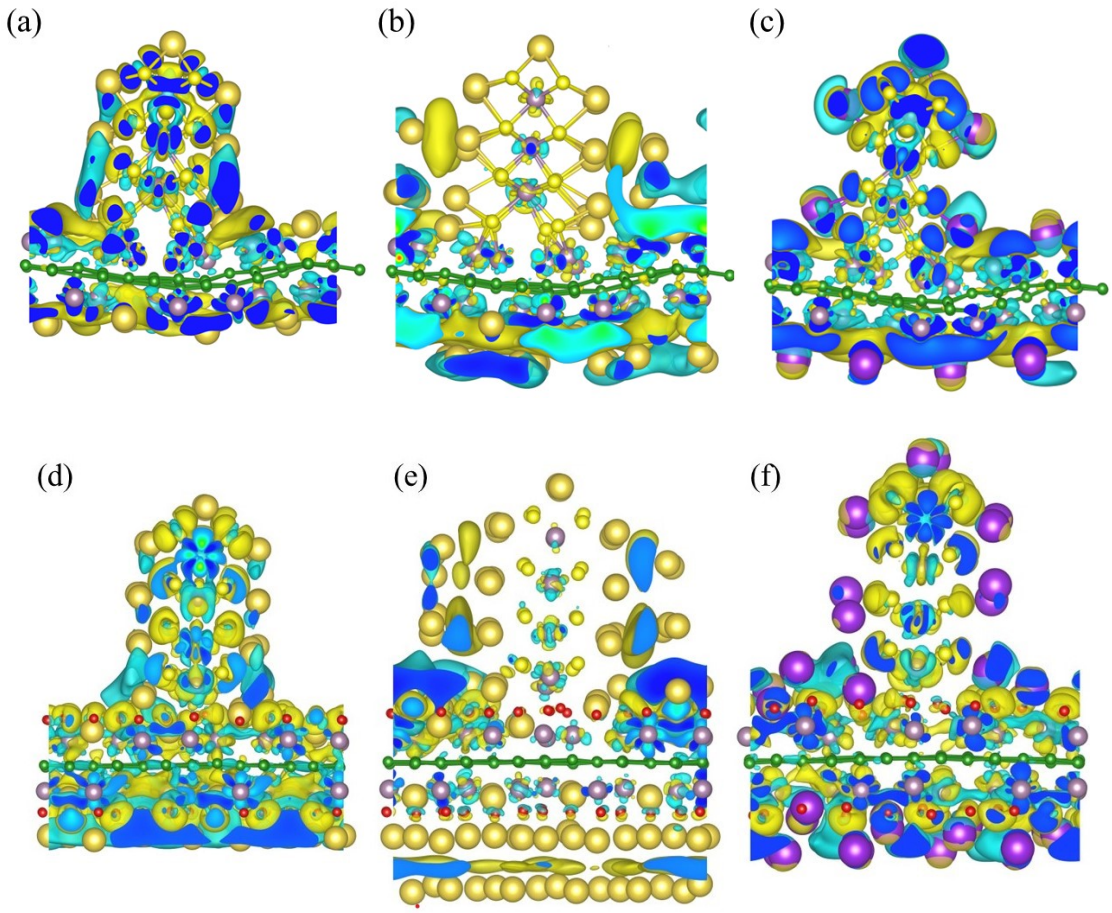

Fig S14 3D-contour plots of the charge density difference at different stages in a multi-layer adsorption process for $MoS_2 \perp Mo_{4/3}B_2$: (a) the first full stable layer of Na^+(0.0020 e $Å^{-3}$); (b) the second full stable layer of Na^+(0.001 e $Å^{-3}$); (c) the first full stable layer of K^+(0.0012 e $Å^{-3}$). For $MoS_2 \perp Mo_{4/3}B_2O_2$: (d) the first full stable layer of Na^+(0.004 e $Å^{-3}$); (e) the second full stable layer of Na^+(0.0012 e $Å^{-3}$); (f) the first full stable layer of K^+(0.003 e $Å^{-3}$).

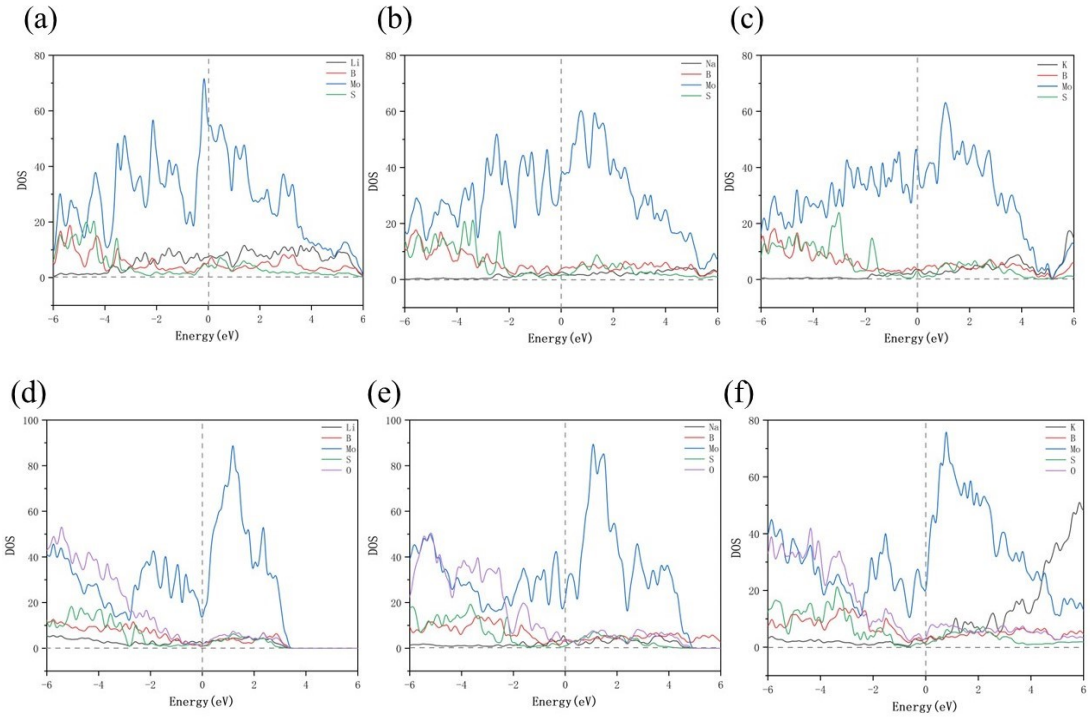

Fig S15 The predicted electronic density of states (DOS) for (a):Li- MoS_2 ⊥ $Mo_{4/3}B_2$; (b):Na- MoS_2 ⊥ $Mo_{4/3}B_2$; (c):K- MoS_2 ⊥ $Mo_{4/3}B_2$; (d):Li- MoS_2 ⊥ $Mo_{4/3}B_2O_2$; (e):Na- MoS_2 ⊥ $Mo_{4/3}B_2O_2$; (f):K- MoS_2 ⊥ $Mo_{4/3}B_2O_2$.

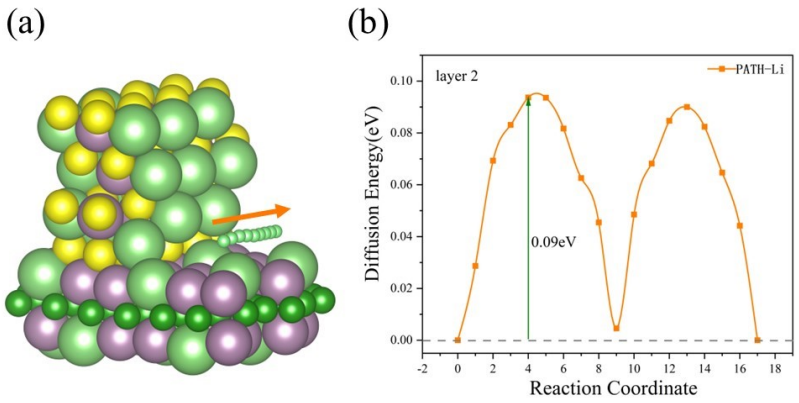

Fig S16 The favorable migration pathway and diffusion energy profile of Li^+ in the second full layer on $MoS_2 \perp Mo_{4/3}B_2$.

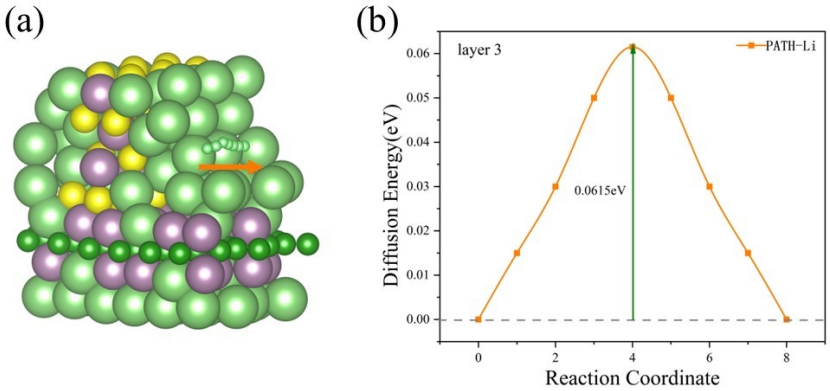

Fig S17 The favorable migration pathway and diffusion energy profile of Li^+ in the third full adsorption layer on $MoS_2 \perp Mo_{4/3}B_2$.

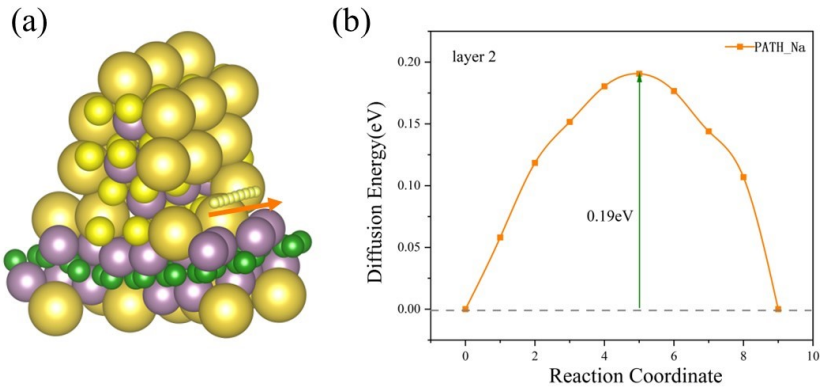

Fig S18 The favorable migration pathway and diffusion energy profile of Na^+ in the second full layer on $MoS_2 \perp Mo_{4/3}B_2$.

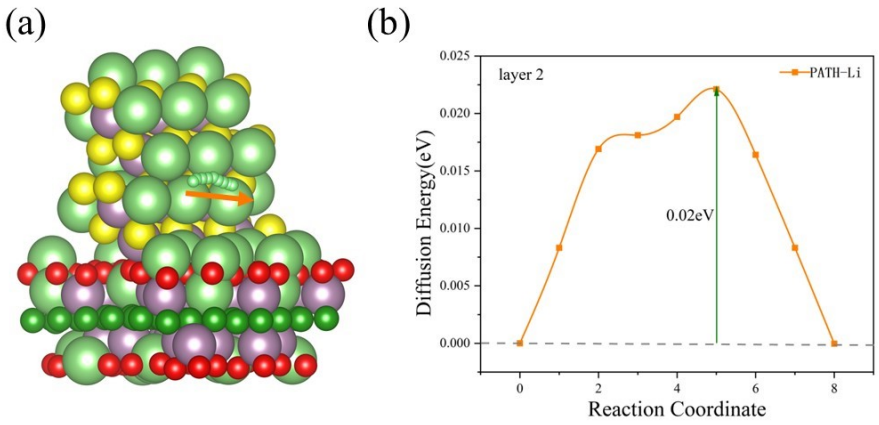

Fig S19 The favorable migration pathway and diffusion energy profile of Li^+ in the second full layer on $MoS_2 \perp Mo_{4/3}B_2O_2$.

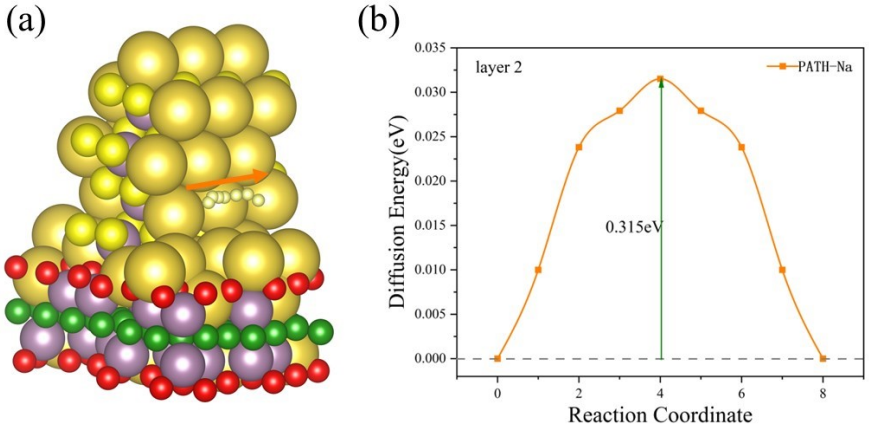

Fig S20 The favorable migration pathway and diffusion energy profile of Na^+ ion in the second full layer on $MoS_2 \perp Mo_{4/3}B_2O_2$.

Table S1 Bader charge analysis of single alkaline metal ion-adsorbed structures of $MoS_2 \perp Mo_{4/3}B_2$ and $MoS_2 \perp Mo_{4/3}B_2O_2$ heterostructures.

		$MoS_2 \perp Mo_{4/3}B_2$					$MoS_2 \perp Mo_{4/3}B_2O_2$					
Site		Mo(b)	B	Mo(m)	S	X	Mo(b)	B	O	Mo(m)	S	X
T_{b1}	Li	0.02	0.27	-	-	-0.82	-1.29	0	0.96	-	-	-0.91
	Na	-0.2	0.27	-	-	-0.73	-1.31	0	0.92	-	-	-0.89
	K	-0.33	0.27	-	-	-0.77	-1.32	0	0.91	-	-	-0.93
T_{b2}	Li	0.11	0.28	-	-	-0.85	-1.26	0	0.96	-	-	-0.91
	Na	-0.12	0.28	-	-	-0.75	-1.27	0	0.92	-	-	-0.89
	K	-0.25	0.28	-	-	-0.79	-1.28	0	0.91	-	-	-0.92
H_{b1}	Li	-0.35	0.32	-	-	-0.85	-1.68	0.37	0.94	-	-	-0.91
	Na	-0.46	0.33	-	-	-0.77	-1.67	0.37	0.91	-	-	-0.88
	K	-0.46	0.31	-	-	-0.79	-1.67	0.37	0.89	-	-	-0.92
H_{b2}	Li	-0.37	0.33	-	-	-0.88	-1.59	0.40	0.93	-	-	-0.9
	Na	-0.42	0.30	-	-	-0.77	-1.67	0.41	0.89	-	-	-0.9
	K	-0.4	0.31	-	-	-0.8	-1.67	0.38	0.88	-	-	-0.93
H_m	Li	-	-	-1.16	0.79	-0.9	-	-	-	-1.16	0.76	-0.91
	Na	-	-	-1.16	0.74	-0.87	-	-	-	-1.16	0.71	-0.89
	K	-	-	-1.16	0.72	-0.9	-	-	-	-1.14	0.7	-0.92
T_m	Li	-	-	-1.15	0.78	-0.89	-	-	-	-1.13	0.76	-0.9
	Na	-	-	-1.15	0.73	-0.87	-	-	-	-1.14	0.7	-0.89
	K	-	-	-1.15	0.7	-0.85	-	-	-	-1.14	0.68	-0.91
Top	Li	-	-	-1.24	0.69	-0.91	-	-	-	-1.24	0.69	-0.91
	Na	-	-	-1.27	0.69	-0.87	-	-	-	-1.27	0.67	-0.87
	K	-	-	-1.29	0.68	-0.88	-	-	-	-1.28	0.66	-0.89
In	Li	-0.77	-	-1.13	0.8	-0.88	-1.68	-	0.96	-1.45	0.65	-0.89
	Na	-0.76	-	-1.13	0.82	-0.83	-1.54	-	0.93	-1.54	0.69	-0.86
	K	-0.75	-	-1.13	0.81	-0.83	-1.3	-	0.89	-1.48	0.67	-0.92